International Journal of Environment and Geoinformatics
2025, 12 (1): 15–27

https://doi.org/10.26650/ijegeo.1569510

Submitted: 28.10.2024
Revision Requested: 21.01.2025
Last Revision Received: 25.01.2025
Accepted: 21.02.2025

International Journal of Environment and Geoinformatics

Research Article

Open Access

Shoreline change monitoring using the Digital Shoreline Analysis System along the coast of Gujarat, India

Foram Jadeja [1] & Kauresh Vachhrajani [2]

[1] The Maharaja Sayajirao University of Baroda, Department of Environmental Studies, Faculty of Science, Gujarat, India
[2] The Maharaja Sayajirao University of Baroda, Department of Zoology, Faculty of Science, Gujarat, India

Abstract

The shoreline is a multifaceted feature of the Earth's surface and is highly susceptible to both natural and anthropogenic influences. Hence, accurate and frequent shoreline change monitoring is essential for determining the dynamic nature of coastal areas. This paper highlights the shoreline changes in the Gujarat coast from 1993 to 2023 with 10-year interval multitemporal Landsat satellite datasets. The modified normalized difference water index was used to extract the shoreline by differentiating the land-water boundary. The shoreline change rates were calculated by applying statistical techniques, such as the end point rate, linear regression rate, net shoreline movement, and weighted linear regression, using a digital shoreline analysis system. In this study, a total of 8782 transects were employed on the considered coastline stretch at an equal distance of 100 meters. Almost half of the transects (49.7%) showed an accretion trend, while erosion was observed in 23.6% of the transects. The remaining 26.7% of transects were in stable condition. This study was performed on a regional scale with significant detailed information that can help further research on sustainable coastal zone management and planning.

Keywords Coastal erosion and accretion · Shoreline change · DSAS · Remote sensing and GIS · Gujarat coast

Citation: Jadeja, F. & Vachhrajani, K. (2025). Shoreline change monitoring using the digital shoreline analysis system along the coast of Gujarat, India. *International Journal of Environment and Geoinformatics*, *12*(1), 15-27. https://doi.org/10.26650/ijegeo.1569510

Corresponding author: Foram Jadeja foram.jadeja-envphd@msubaroda.ac.in

Introduction

The shoreline is considered as the boundary between terrestrial and marine realms and undergoes constant changes due to complex interactions through various affecting factors, such as wave energy, wind speed and wind direction, tidal amplitude and frequency, and sea level fluctuations. Shoreline changes occur over a wide spectrum of temporal scales with natural and anthropogenic activities. The procurement of coastal sand through mining, over-exploitation of groundwater, reclamation of land, and various human-induced coastal developmental activities contribute to the negative impact on the environment, which ultimately leads to coastline retreat. Short-term coastal morphological changes occurring over relatively brief timescales ranging from seasonal to multiannual periods are mostly forced by nearshore hydrodynamic phenomena, including fluvial discharge, waves, storms, tidal currents, and sea level anomalies (Buırak et al., 2004; Splinter et al. 2014; Coco et al. 2014). However, chronic changes along the coast are often attributed to long-term processes spanning from decades to centuries, encompassing sediment supply (forces of erosion, deposition, and sediment transport), varying relative sea levels, changes in land-use patterns, and fluctuations in climatic conditions (Vitousek et al. 2017). Shoreline change detection plays a crucial role in various disciplines, including coastal zone management, flood prediction, and coastal erosion and accretion monitoring, and facilitates policy-making and decision-making processes (Giardino et al. 2010; Gazioğlu, 2018). Therefore, assessments of dynamic shoreline changes are essential.

Li and Ma (2001) stated that the shoreline is a highly distinctive characteristic of the Earth's surface. It is one of the twenty-seven characteristics acknowledged by the International Geographic Data Committee. The scientific community became interested in this issue over a decent amount of time, and numerous research studies have been conducted to explore and quantify fluctuating shorelines across the globe. In many coastal countries, assessments of shoreline change have been conducted using either digital shoreline analysis systems or conventional mapping. Remote sensing data and geographical information system (GIS) techniques are indispensable tools for mapping and monitoring large-scale shoreline information at lower costs and in less time. For shoreline shift analysis, several researchers have used various GIS tools and satellite image analysis techniques based on band ratio, band difference, single band threshold, and post image pixel classification (Çelik & Gazioğlu, 2020; El-Asmar and Hereher 2011; Hossain et al. 2021). In geospatial research, a prerequisite for shoreline delineation necessitates the inclusion of both water and land sections as contrasting elements in satellite images. Consequently, water indices are being developed and utilized to distinguish between land and water. The normalized difference water index (NDWI) (McFeeters 1996), modified normalized difference water index (MNDWI) (Xu 2006), water ratio index (WRI) (Shen and Li 2010), and automated water extraction index (AWEI) (Feyisa et al. 2014) facilitate the separation of land–water boundaries to extract clear shorelines. Recent advancements in coastal geospatial research have led to automatic and semiautomatic shoreline delineation (Hossain et al. 2021). Various algorithms have been formulated for the retrieval of coastline information from satellite images. Alesheikh et al. (2007) introduced the concept of utilizing band ratio analysis for automatic demarcation of the shoreline. Braud and Feng (1998) and Frazier and Page (2000) used Landsat satellite images to identify and extract shorelines by employing various techniques of image analysis, including density slicing. However, Guariglia et al. (2006) and Ustun et al. (2004) used supervised and unsupervised classification methods. Chen et al. (2019) developed a method in which the greenness and wetness components of the tasseled cap transformation were used to extract coastlines. Hossain et al. (2021) adopted the NDWI and Canny edge detection methods to retrieve coastal information. The majority of the research has used both automatic and manual digitizing approaches to extract shorelines.

The continuous erosion of the global shoreline occurs at varying rates, ranging from 0.01 to 10 m/year (CERC 1984; Pilkey and Hume 2001). Many researchers worldwide have examined the spatiotemporal variations in shorelines through both qualitative and quantitative analysis techniques (Addo et al. 2011; Kabuth et al. 2014; Tran Thi et al. 2014; El-Sharnouby et al. 2015). The Digital Shoreline Analysis System (DSAS), an extension of ArcGIS software, has been widely used to determine the net rate of change in shoreline position using various statistical methods, such as the end point rate (EPR), linear regression rate (LRR), and weighted linear regression rate (WLR) (Thieler et al. 2009; Himmelstoss et al. 2018). Nassar et al. (2019) measured the shoreline variation along the North Sinai coast in Egypt using the DSAS tool. Yan et al. (2021) studied the temporal and spatial variation in the shoreline and reported an 8% erosion rate on the Yancheng coast, China. The spatiotemporal changes in the short- and long-term characteristics of the shoreline of João Pessoa city, Brazil, were also examined using the DSAS technique (Santos et al. 2021).

In India, studies have been conducted to evaluate the coastal vulnerability index by considering factors such as coastal slope, coastal geomorphology, shoreline change rate, tidal height, and wave height for various maritime states, such as Andhra Pradesh (Basheer Ahammed et al. 2016), Orissa (Kumar et al. 2010; Roy et al. 2018), Kanyakumari and Tuticorin of Tamil Nadu (Mujabar and Chandrasekar 2013), Kerala (Mohan and Jairaj 2014), and Karnataka (Beluru Jana and Hegde 2016). Jayanthi et al. (2018) assessed shoreline changes and potential sea level rise impacts on the southeastern coast of India. Ratheesh et al. (2023) quantified the shoreline change across the entire Indian coast (7549 km) between 2004-2006 and 2014-2016 and observed erosion along 1144 km and accretion along 1084 km, whereas 5321 km of the coastline exhibited no changes. Kankara et al. (2018) published a status report for 26 years (1990–2016) of shoreline changes along the whole Indian coast covering every maritime state. For the Gujarat coast, shoreline change assessment results from 1990 to 2016 revealed that 43% of the coast is stable, 31% is eroding, and the remaining 26% is accreting (Kankara et al. 2018). Misra & Balaji (2015) predicted high rates of erosion of approximately 4 m/year for the coastal states Surat, Navsari, and Valsad of southern Gujarat.

The understanding of the intricate processes of accretion and erosion in coastal regions relies heavily on the analysis of shoreline shifts. The focus of this study will be on quantifying alterations in the coastal shoreline and identifying the underlying mechanisms that have contributed to these changes over the past 30 years in the coastal region of Gujarat, i.e., the Saurashtra Coast, Gulf of Khambhat, and South Gujarat Coast. A long-term analysis, i.e., a multidecadal study through remote sensing datasets, will shed light on valuable insights and vulnerability. Such awareness will aid in understanding the complex dynamic changes in the Gujarat coast. The aims of the study are as follows:

(a) To examine the spatial and temporal variations of Gujarat's coastline along with two union territories between 1993 and 2023 using RS and GIS techniques.

(b) Quantification of the rate of shoreline change with multiple regression techniques, i.e., EPR, NSM, WLR, and LRR, to appropriately analyze the statistical techniques for determining the rate of shoreline change.

(c) To classify the coastal stretch based on the rates of shoreline changes into erosion, accretion, and constant.

(d) To Identify the accretion and erosion rate through observing and interpreting multi-decadal coastline changes.

This investigation might assist coastal researchers and decision-makers in their pursuit of future studies, management, and sustainable development and planning of coastal zones.

Study Area

The coastline of Gujarat is approximately 1650 km long. It is below the 30-meter contour line above sea level, so it is categorized as a low-lying terrain, thus making it susceptible to erosion. Gujarat has the longest coastline in the country and extends from the Kachchh district to the Valsad district, covering 14 coastal districts and 2 union territories (Sutariya et al., 2021). The Gujarat coast has been broadly classified into five regions: (i) the Rann of Kachchh, (ii) the Gulf of Kachchh, (iii) the Saurashtra Coast, (iv) the Gulf of Khambhat, and (v) the South Gujarat Coast. Gujarat has two gulfs, the Gulf of Kachchh and the Gulf of Khambhat, along its coastline. The strong semidiurnal tides with high tidal ranges and associated currents are responsible for the formation of the gulf's depositional and erosional features. The coast of Gujarat comprises diverse ecosystems, including estuaries, rivers, islands, mudflats, beaches, terraces, cliffs, plains, coral reefs, and mangroves. Figure 1 shows that in the present study, 12 coastal districts, i.e., Devbhumi Dwarka, Porbandar, Junagadh, Gir Somnath, Amreli, Bhavnagar, Ahmedabad, Anand, Bharuch, Surat, Navsari, and Valsad, covering the Saurashtra Coast, Gulf of Khambhat, and the southern Gujarat Coast, are selected as the study area. Two union territories, Diu and Daman, are also considered a part of the study due to their geographical location, which coincides with the continuation of the Gujarat coastline.

Materials and Methodology

Data Sources

To study shoreline shifts over the past three decades (1993-2023), multitemporal Landsat satellite images were used. This research examined four different scenes with 10-year intervals (1993/2003/2013/2023) to observe the movement of the coastline. The Landsat MSS, TM/ETM+, and OLI images were downloaded from https://earthexplorer.usgs.gov/, corresponding to the path/row number of the satellite covering the Gujarat coast. The details of the Landsat digital data acquired are given in Table 1. Landsat-5 TM (Thematic Mapper) data include a total of 7 channels covering the visible spectrum (1 to 3) and near-infrared (NIR) wavelengths (channel 4) and 5 and 7 channels covering the mid-infrared (MIR), while the thermal infrared (TIR) is covered by channel 6. Landsat 7 carries the Enhanced Thematic Mapper Plus (ETM+) sensor, which contains eight spectral bands, including a pan and a thermal band. Landsat 8 carries two instruments: the Operational Land Imager (OLI) and the Thermal Infrared

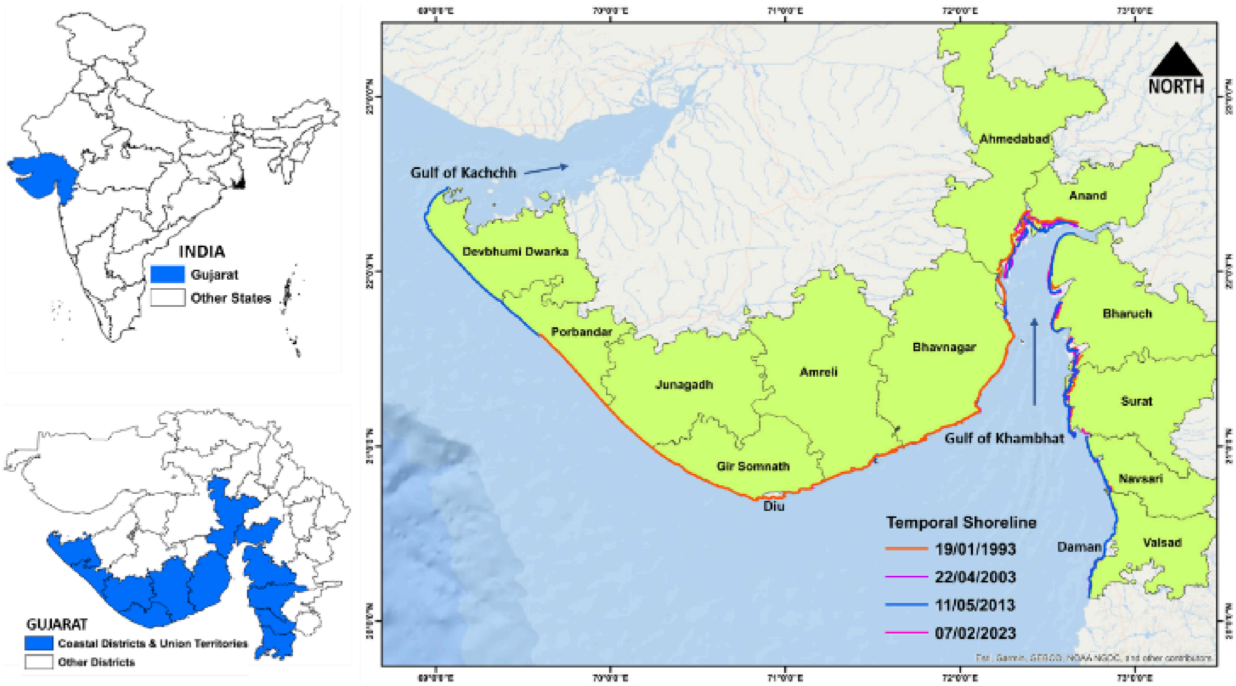

Figure 1. Location map of the study area.

Sensor (TIRS). The OLI sensor provides enhancement from the earlier ETM+ sensor, with the addition of two new spectral bands, i.e., a deep blue VIS channel 1 and a new channel 9 infrared band (https://www.usgs.gov/landsat-missions/). All the acquired satellite images for the research had less than 10% cloud coverage within the study area.

Preprocessing of satellite images

First, the collection of satellite images was checked against striping/missing data. All Landsat data are generally processed as Level 1 terrain corrected (L1T) data, which offers systematic radiometric and geometric accuracy. The images were processed in freely available QGIS software. For the generation of false color composite (FCC) images, band 2, band 3, and band 4 were used for Landsat TM and Landsat ETM, whereas band 3, band 4, and band 5 were used for Landsat 8 via the layer stacking method. All data used in this study are ortho-rectified products. Essentially, they are in the Universal Transverse Mercator (UTM) projection system and the World Geodetic System (WGS-84) datum.

Table 1. Details of the Landsat multispectral data acquired from 1993 to 2023

Satellite/Sensor	Spatial Resolution (m)	Path/Row	Acquisition Date
Landsat 5/TM	30	148/045, 148/046,	19/1/1993
Landsat 7 /ETM		149/045, 149/046,	22/4/2003
Landsat 8 /OLI_TIRS		150/045, 151/044,	11/5/2013
Landsat 8 /OLI_TIRS		151/045	07/2/2023

Shoreline Indicator

Several shoreline indicators exist, notably, the vegetation line, high water line, mean water line, low water line, high tide line, etc., which are not necessarily visible to the human eye. Thus, various image processing techniques have been employed to extract shorelines from satellite images based on elevation variation, moisture content, etc. In dynamic ecosystems, a high water line provides a pragmatic approach for deriving shorelines from land–water boundaries in evolving environments (Pajak and Leatherman 2002).

Shoreline detection and extraction

Land-water boundary extraction can be performed by applying various water indices using a band ratio between two spectral bands. The NDWI is widely used for water body mapping, where green and NIR spectral bands have been used to effectively enhance water information. Water bodies absorb visible to infrared wavelengths and reflect low radiation. This technique has been modified to obtain more enhanced water features by substituting the SWIR band instead of the NIR band. Figure 2 shows that, in the present study, the modified normalized difference water index (MNDWI) was utilized to detect and extract the water features as well as to obtain the land–water boundary (Xu 2006). It can be expressed as follows:

MNDWI= (Green – SWIR) / (Green + SWIR)

Negative pixel values close to −1 represent land features, while pixels representing water features have positive values

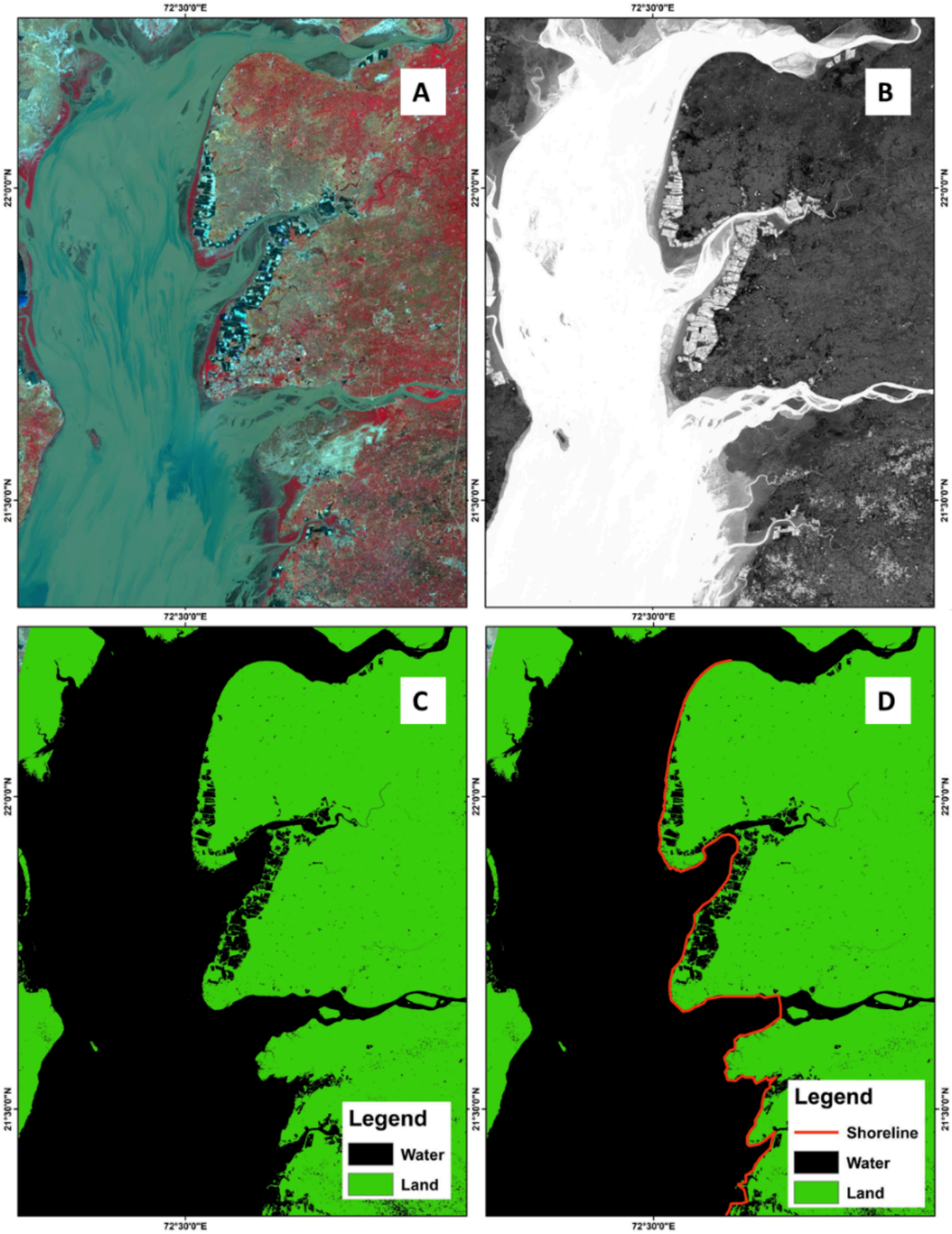

Figure 2. Example of shoreline extraction from satellite images via MNDWI and binary image conversion (the depicted area is part of the Gulf of Khambhat): (A) FCC image, (B) MNDWI raster, (C) binary raster, and (D) shoreline from the raster binary

close to +1. The MNDWI raster was used to separate the water zone from the terrain. The water region was removed as a binary image using the spatial analyst tool in ArcGIS software. Then, from the extracted water binary images, shorelines were manually digitized for all consecutive years. The extracted shoreline was smoothed and further updated from the satellite image because, in certain areas, the shoreline was not generated accurately due to image distortion.

Estimation of Shoreline Changes

The digital shoreline analysis system (DSAS) is an open-source software extension of ArcGIS software developed by

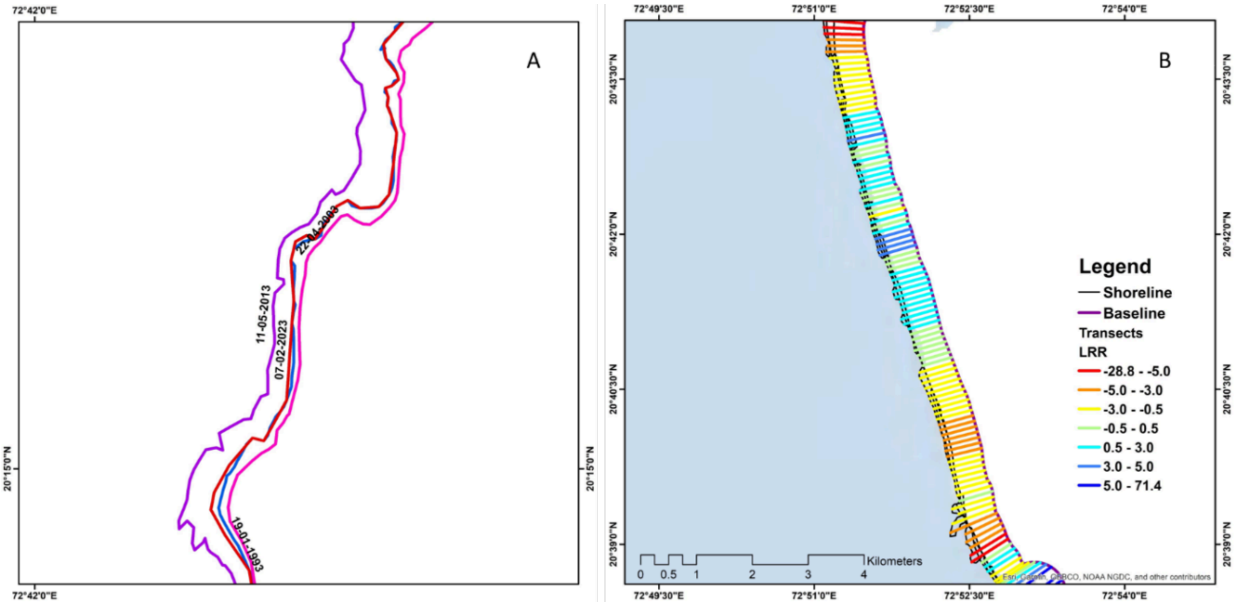

Figure 3. A: Temporal shorelines (merged) with required attributes (geo-database), B: Transects along with the shoreline and baseline

the United States Geological Survey (Thieler et al. 2009). This extension tool analyses the shoreline change rate using statistical calculations from the time series of shoreline vector data. After the creation of the database, the shoreline feature was manually defined based on a visual tonal difference between the land and water pixels from the binary image at a scale of 1:25000. The temporal shorelines (1993, 2003, 2013, and 2023) were merged into a feature class with the required attributes (Figure 3A). To create a baseline, the buffer operation was carried out on the merged shoreline. The baseline on the landward side is a parallel reference line to the set of historical shorelines. The transects were cast at equal intervals of 100 meters on the entire coastline, which were perpendicular to the baseline (Figure 3B). The change rate statistics for a time-series shoreline were computed using the distance from the baseline to each intersection point of the transect.

The DSAS tool provides various statistical measurement methods for shoreline change calculations. These include the net shoreline movement (NSM), shoreline change envelope (SCE), end point rate (EPR), linear regression rate (LRR), and weighted linear regression rate (WLR) (Himmelstoss et al. 2018). The NSM measures the distance between the oldest and the youngest shorelines for each transect. The SCE value refers to the distance within the entire shoreline intersects for every transect. The distance of shoreline movement divided by the time elapsed between the oldest and the current shoreline yields the end point rate. The LRR can be determined by fitting a least-squares regression line to all shoreline points for a transect, whereas the WLR was used to calculate the rate of change involving more than two periods of shoreline positions by plotting a least-squares regression line. Figure 4 illustrates the methodology adopted for the study.

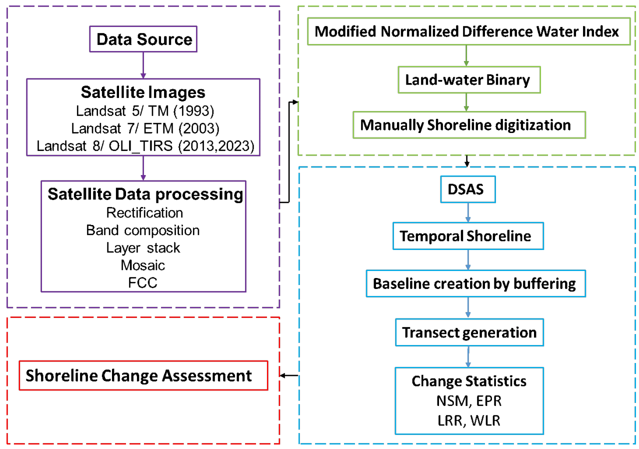

Figure 4. Schematic representation of the overall methodology used for the execution of research.

Results and Discussion

The present study assessed shoreline changes along the twelve coastal districts of Gujarat and two union territories using data derived from multidated satellite images over the past three decades (1993-2023). The DSAS tool was used to estimate the shoreline change and rate calculation. Three statistical measures (EPR, LRR, WLR) were calculated for the rate of change along the shoreline, and NSM was used for the distance measurements. The results of the present study are compiled and summarized in Table 2, where negative values indicate erosion and positive values indicate accretion.

Table 2. District-wise shoreline change rate classification distribution

District	Shoreline considered for mapping (km)	High Erosion	Moderate Erosion	Low Erosion	Stable Coast	Low Accretion	Moderate Accretion	High Accretion
Devbhumi Dwarka	100	0.1	1	30.6	50.7	17.5	0.1	0
Porbandar	89	0	0	7.9	36	44.6	0.2	0.3
Junagadh	32	0	0	4.3	12.8	14.9	0	0
Gir Somnath	108.7	0.4	1.2	17.9	49	39.4	0.4	0.4
Amreli	58.2	3	2.2	9.1	10.9	23.9	2.4	6.7
Bhavnagar	151.8	16.4	4.9	24.1	41	30.2	8	27.2
Ahmedabad	32.1	11	0	0.3	0	0	0	20.8
Anand	32.1	1.7	0	0.1	0	0.2	0.6	29.5
Bharuch	95.1	10.7	1.2	2	2	13.9	6.7	58.6
Surat	48.5	4.8	2.1	1.4	1.5	2.4	2.3	34
Navsari	42.7	3.7	5.1	10.3	4.5	7	3.9	8.2
Valsad	63.6	2.3	5.2	19.6	11	16	4.7	4.8
Daman*	12.1	0	0	2.2	4.3	3.8	1.7	0.1
Diu*	12.3	0	0	0.8	10.4	1	0	0.1
Total	878.2	54.1	22.9	130.6	234.1	214.8	31	190.7

**Union Territories*

Erosion and accretion trends were determined based on linear regression. The LRR values have been used to classify coastal stretches into seven categories (Table 3) based on the rates of shoreline change (Kankara et al. 2018):

A total of 8782 transects were laid upon the considered coastline stretch of 878.2 kilometers at an equal distance of 100 meters. Half of the transects (49.7%, 436.5 km) showed accretion, while erosion was observed on 23.6% (207.6 km) of the coast. The remaining 26.7% (234.1 km) of the coast showed no significant changes (Figure 5). The detailed change rate characterization and erosion-stable-accretion status (in percentages) distributions among the coastal districts and union territories are given in Table 4 and Figure 5, respectively. Since 1993, the coastal stability of Diu has been consistently high, at approximately 85%, preceding that of Devbhumi Dwarka and Gir Somnath, at 51% (50.7 km) and 45% (49 km), respectively. However, Ahmedabad, Anand, Bharuch, and Surat exhibited no signs of coastal stability. The erosion history revealed that the coastlines of Navsari and Valsad eroded approximately 43-45% of the coast on the southern coast of Gujarat. Over the years, the coastal districts of Anand, Bharuch, Surat, and Ahmedabad have experienced significant accretion, Anand with a peak rate of 94% over 30.3 km. Bharuch follows closely, with an accretion of 83% at a distance of approximately 79.2 km. The accretion rate of the surat was 80% (38.7 km), while that of the Ahmedabad accreted at 65%. These districts have experienced notable changes in landforms due to the accumulation of sediments and other materials along their coasts. Out of the total coastline of 878.2 km, a significant portion of 54.1 km experienced high erosion, 22.9 km experienced moderate erosion, and 130.6 km experienced low erosion. On the other hand, a relatively small stretch of 31 km experienced moderate accretion, with 190.7 km of high accretion, while a distance of 214.8 km exhibited low accretion. The remaining 234.1 km of the coastline remained stable and unaffected by any changes. The shorelines in Gujarat are changing differently. The Saurashtra coast has a stable shoreline, while the southern coast of Gujarat is experiencing erosion (Ratheesh et al. 2023).

Devbhumi Dwarka

Devbhumi Dwarka is the westernmost district of Gujarat and is located on the southern coast of the Gulf of Kachchh. The western coastline of the district covers a distance of 100 km. Overall, 51% of the coast is stable, with 18% accretion and 32% erosion (Figure 5). The NSM values for maximum accretion and erosion are 105.61 m and −203.64 m, respectively. The EPR and WLR values for the minimum regressive and progressive shorelines are −0.01 m/y and 0.01 m/y, respectively, whereas the corresponding maximum values are −10.03 m/y and 3.51 m/y (EPR) and −10.07 m/y and 3.2 m/y (WLR), respectively. Devbhumi Dwarka has the most stable coastline of Gujarat state, with a stable coastal stretch of approximately 51 km.

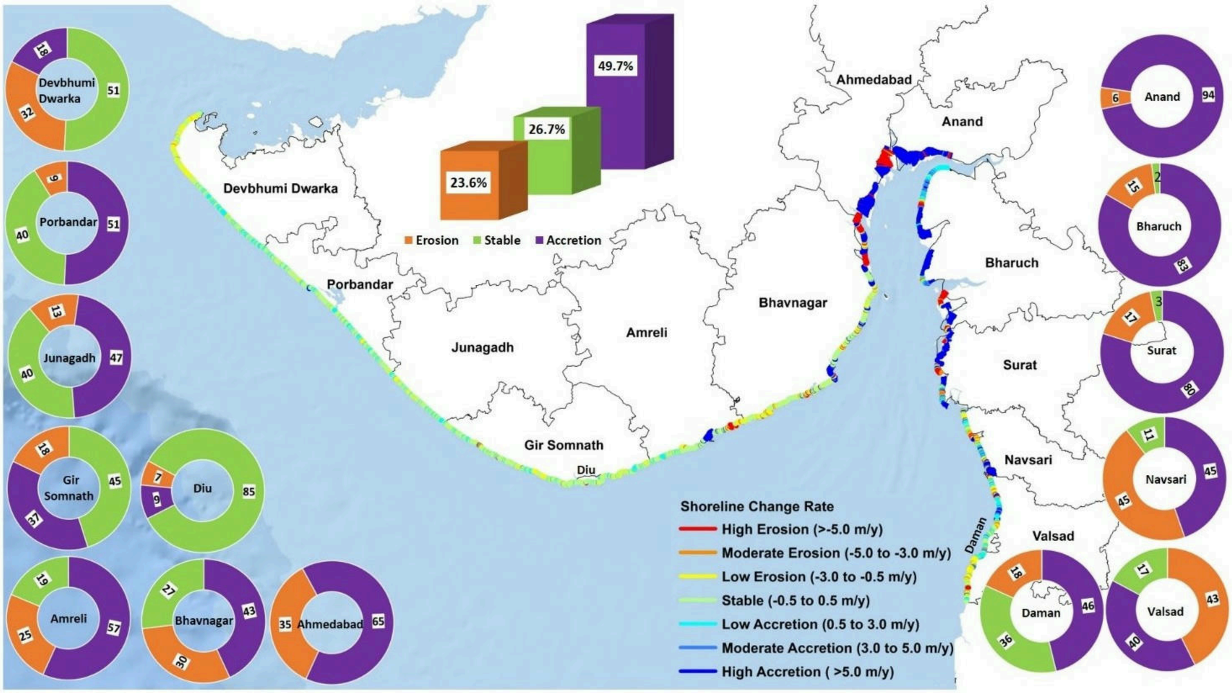

Figure 5. Map of shoreline change rate classification with total erosion, stable, and accretion

Porbandar

Approximately 89 km of the long coastline covered by the Porbandar district is dominated by low accretion of approximately 45 km. Forty percent of the coast exhibited no significant change, covering 36 km of the district. Porbandar is one of the least eroding districts, representing only 9% of the total area. The average accretion and erosion NSM values of Porbandar were 18.98 m and -8.89 m, respectively. The EPR and WLR values for the maximum regressive shoreline change were −1.5 and −1.49 m/y, respectively, while the rates for the maximum progressive change were 8.19 and 7.39 m/y, respectively.

Junagadh

The Junagadh coast has not experienced a moderate to high erosion/accretion trend. The min/max NSM values of accretion are 0.01 m/57.93 m, whereas they are −0.09 m/-37.57 m for the erosional trend. The maximum EPR values for progressive and regressive shoreline changes were 1.93 m/y and −1.25 m/y, respectively. The maximum WLR values are 1.57 m/y and −1.39 m/y, respectively. A total of 320 transects were employed on the coastline of the entire district (32 km), of which 149 transects experienced an accretion trend, while 128 transects remained in stable condition. This indicates that 13% of the coast has receded, while 47% and 40% of the Junagadh coastlines have experienced accretion and stabilized states, respectively.

Gir Somnath

The district covers approximately 109 kilometers of extensive shoreline. Among these, 45% (49 km) are the stable coast of Gir Somnath, where 37% have an accretion trend (39.4 km of low accretion, 0.4 km of moderate or high erosion), and 18% of the coast exhibits an erosional trend. The average NSM values for the Gir Somnath district are 20.73 m (accretion) and −19.22 m (erosion). The maximum end point rates are 8.28 m/y and −43.19 m/y, and the WLR values are 7.26 m/y and −11.38 m/y, where positive values indicate accretion and negative values indicate degradation.

Amreli

The Amreli coast covers an approximately 58 km long coastline. To assess the changes in the coastline over time, a total of 580 transects were established across the entire stretch. Among the 330 transects (57%) that experienced accretion, 19% (109 transects) of the transects showed no change, whereas 143 transects were eroded (25%). The maximum net shoreline movement values for the Amreli coast were 1492.42 m and −1440.8 m, respectively. The maximum progressive EPR/WLR values are 143.35 m/y and 73.74 m/y, respectively. The −43.19 m/y and −11.38 m/y rates represent the maximum regression rates of the EPR and WLR, respectively, of Amreli.

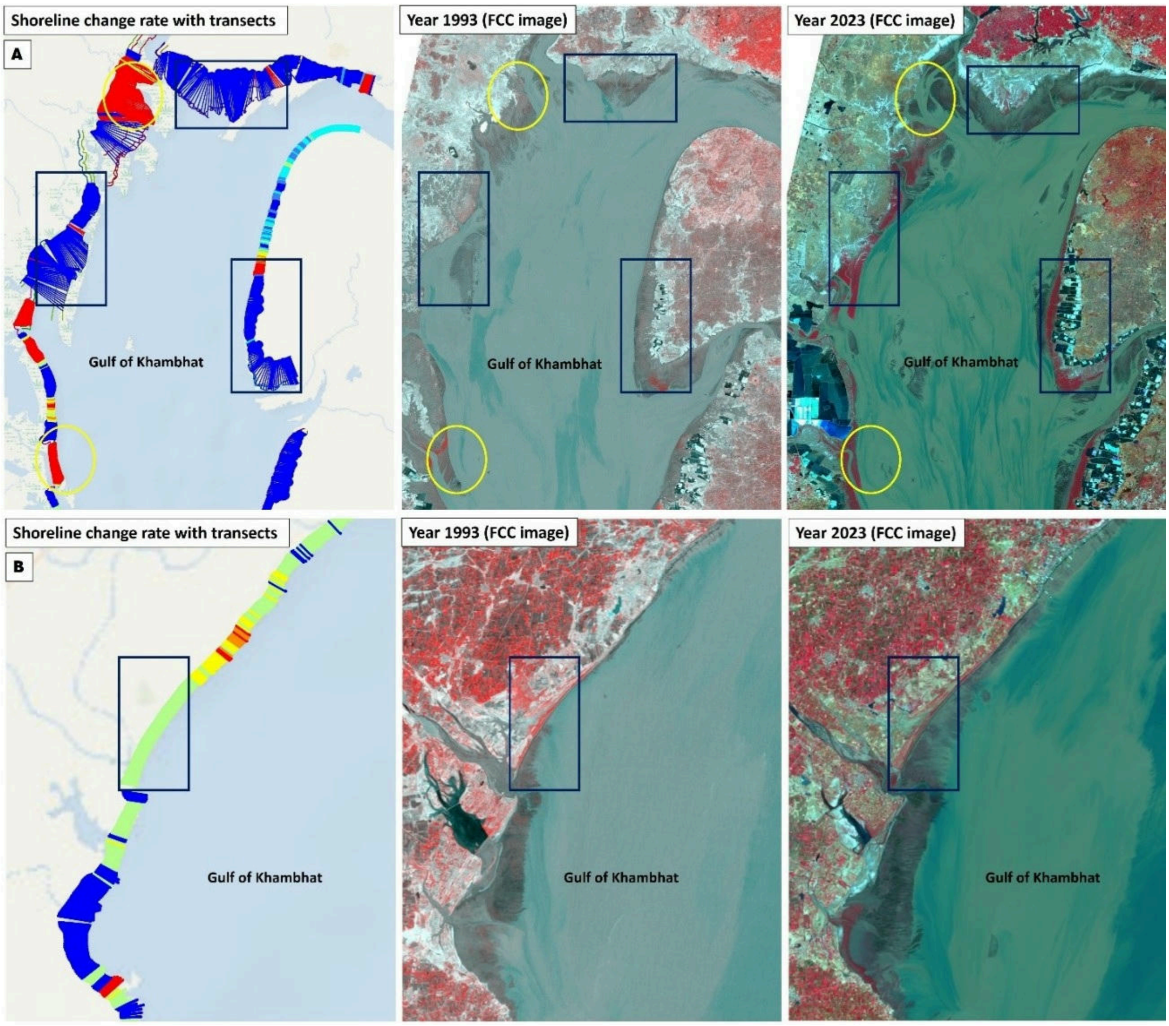

Figure 6. Enlarged view of shoreline change rate classification with FCC images (In Figure 6A, the square box indicates the areas experiencing accretion, while the circle highlights the regions exhibiting erosion trends along various sections of the Gulf of Khambhat. In Figure 6B, the square box emphasizes the stable shoreline pattern observed consistently from the year 1993 to 2023.

Bhavnagar

The Bhavnagar coast has the longest coastline among all the districts considered in the study area, measuring approximately 152 kilometers. The average net shoreline movement values are 168.56 m/-175.39 m, whereas 1078.86 m/-1458.43 m are the maximum NSM values of the Bhavnagar coastline. 0.01 m/y and -0.01 m/y (min EPR), 53 m/y and -58.37 m/y (max EPR), 0.01 m/y and -0.01 m/y (min WLR), and 53.34 m/y and -53.8 m/y (max WLR) are the shoreline change rates of the Bhavnagar coast. It has been found that approximately 43% of the coast, which is around 65 km in length, has followed the accretion trend. Out of this, about 30 km is covered by low accretion, while the remaining 27 km of the coast is highly accreted. On the other hand, 27% of the coast has remained unchanged over time. However, it has been observed that around 45.4 km of the coast is still experiencing erosion, which is a matter of concern for the Bhavnagar district.

Table 4. Shoreline change rate classification

Categories	Rate (m/year)	Color code
High Erosion	< -5.0	
Moderate Erosion	-5.0 to -3	
Low Erosion	-3.0 to -0.5	
Stable Coast	-0.5 to 0.5	
Low Accretion	0.5 to 3.0	
Moderate Accretion	3.0 to 5.0	
High Accretion	> 5.0	

Anand

The coastline considered for shoreline change in the Anand district was about 32 km long. Among the 12 coastal districts and 2 union territories, notably, Anand district has witnessed the highest accretion trend of about 94% (29.5 km). The district's maximum NSM accretion value is 5489.16 m, while its erosional NSM value is -963.32 m. The maximum EPR and

Table 3. Statistical synthesis of the study area during (1993–2023)

The Gujarat Coast															
	Devbhumi Dwarka	Porbandar	Junagadh	Gir Somnath	Amreli	Bhavnagar	Ahmedabad	Anand	Bharuch	Surat	Navsari	Valsad	Daman	Diu	Total
Total number of transects	1000	890	320	1087	582	1518	321	321	951	485	427	636	121	123	8782
Shoreline length (km)	100	89	32	108,7	58,2	151,8	32,1	32,1	95,1	48,5	42,7	63,6	12,1	12,3	878,2
(NSM)min accretion (m)	0,03	0,03	0,01	0,05	0,07	0,01	42,25	0,92	5,11	0,04	0,59	0,1	0,64	0,22	50,07
(NSM)min erosion (m)	−0,01	−0,03	−0,09	−0,01	−0,02	−0,03	−30,57	−0,37	−2,57	−2,58	−0,03	−0,02	−1,71	−0,06	−38,1
(NSM) avg accretion (m)	19,29	18,98	12,26	20,73	201,49	168,56	2639,86	1481,49	955,29	1199,71	303,96	82,34	59,87	20,68	7184,525
(NSM) avg erosion (m)	−27,63	−8,89	−11,03	−19,22	−129,02	−175,39	−2112,75	−236,18	−556,96	−216,3	−169,24	−185,42	−17,57	−4,83	−3870,16
(NSM) max accretion (m)	105,61	246,11	57,93	248,81	1492,42	1078,86	6257,29	5489,16	3884,55	3948,41	1924,89	2231,69	253,31	208,25	27427,29
(NSM) max erosion (m)	−203,64	−38,61	−37,57	−855,13	−1440,84	−1458,43	−4121,79	−963,32	−1808,73	−693,49	−1967,17	−6204,74	−60,81	−18,16	−19872,4
Minimum progressive shoreline change rate (m/year)															
EPR	0,01	0,01	0,01	0,01	0,01	0,01	1,41	0,03	0,17	0,06	0,02	0,01	0,02	0,01	1,79
LRR	0,01	0,01	0,01	0,01	0,01	0,01	8,13	1,65	0,21	0,07	0,03	0,01	0,02	0,01	10,19
WLR	0,01	0,01	0,01	0,01	0,01	0,01	8,13	1,65	0,21	0,07	0,03	0,01	0,02	0,01	10,19
Minimum regressive shoreline change rate (m/year)															
EPR	−0,01	−0,01	−0,01	−0,01	−0,01	−0,01	−1,02	−0,01	−0,09	−0,11	−0,02	−0,01	−0,06	−0,01	−1,39
LRR	−0,01	−0,01	−0,01	−0,01	−0,01	−0,01	−1,96	−0,97	−0,01	−0,13	−0,02	−0,01	−0,02	−0,01	−3,19
WLR	−0,01	−0,01	−0,01	−0,01	−0,01	−0,01	−1,96	−0,97	−0,01	−0,13	−0,02	−0,01	−0,02	−0,01	−3,19
Maximum progressive rate shoreline change rate (m/year)															
EPR	3,51	8,19	1,93	8,28	143,35	53	237,51	194,22	163,9	131,39	64,05	74,26	8,43	6,93	1098,95
LRR	3,2	7,39	1,57	7,26	73,74	53,34	237,54	217,17	164	129,23	71,43	81,39	6,51	5,5	1059,27
WLR	3,2	7,39	1,57	7,26	73,74	53,34	237,54	217,17	164	129,23	71,43	81,39	6,51	5,5	1059,27
Maximum regressive rate shoreline change rate (m/year)															
EPR	−10,03	−1,5	−1,25	−43,19	−47,94	−58,37	−188,18	−48,66	−60,19	−23,08	−65,46	−206,47	−2,02	−0,6	−756,94
LRR	−10,07	−1,49	−1,39	−11,38	−56,51	−53,8	−188,5	−47,45	−60,84	−22,9	−70,95	−195,65	−1,82	−1,57	−724,32
WLR	−10,07	−1,49	−1,39	−11,38	−56,51	−53,8	−188,5	−47,45	−60,84	−22,9	−70,95	−195,65	−1,82	−1,57	−724,32
Total transects that record accretion															
LRR	176	451	149	402	330	654	208	303	792	387	191	255	56	11	4365
Total transects that record erosion															
LRR	317	79	43	195	143	454	113	18	139	83	191	271	22	8	2076
Total transects that record accretion stabilization															
LRR	507	360	128	490	109	410	0	0	20	15	45	110	43	104	2341

LRR values for progressive shoreline change were 194.22 m/y and 217.17 m/y whereas -48.66m/y and -47.45m/y are the maximum regressive values of shoreline change. According to recent observations, there has been a complete absence of stability observed along the coastline of the Anand district. This lack of stability may be a cause of concern and requires further investigation and analysis to determine the underlying causes and potential solutions.

Bharuch

The Bharuch district is located in the eastern part of the Gulf of Khambhat. A coastline stretch of about 95 kilometers was considered for the shoreline change detection analysis. The minimum and maximum accretion net shoreline movement values are 5.11 m and 3884.55 m while the -2.57 m and -1808.73 m are the min. and max. erosion NSM values of the Bharuch coast. It is the second most highly accreted coast, covering 83% of the total stretch, including a high accretion of about 58.6 km at the center and southern part of the district, while a low to moderate accretion of 20.6 km was mainly observed at the northern coast of the district. Dey et al. (2021) also observed an accretion trend between 2012 and 2021 while monitoring the Dahej coast, which is located in the central region of the Bharuch district. Approximately 14 km (15%) of the coastline has been eroded with the low to high erosional pattern, while 2% of the total coastline has remained the same. The Bharuch district's maximum progressive and regressive EPR and WLR values are 163.9 and 164 m/y and -60.19 and -60.84 m/y, respectively.

Surat

About 49 km long shoreline was considered for the change analysis of the Surat district. Over the years, 34 km (80%) of the coast has experienced a significant increase in land deposition, indicating a highly accreting area in the northern part of the district. However, 17% (8.3 km) of the coast is experiencing erosion at a maximum rate of -22.9 m/y (LRR). Only 2% of the total coastline remained the same. The maximum accretion and erosional net shoreline movement of the Surat district were 3948.41 m and -693.49 m. 131.39 m/y (EPR) and 129.23 m/y (LRR) are the maximum progressive shoreline change rate of the coast. Misra and Balaji (2015) also observed an accumulation pattern at the north of Hazira port. The strong tidal currents and substantial loads of sediments associated with the major river could be responsible for the accumulation pattern on the dynamic coastline (Gupta 2014).

Navsari

The Navsari district has a coastline stretch of about 43 kilometers. From which approx. 45% of the coast is eroding while another 45% has shown an accretion trend. Only a small stretch of 4.5 km, which covers about 11% of the total area, has remained unchanged. The noted average NSM values for erosional and accretion trends are -169.24 m and 303.96 m, respectively. The maximum WLR and EPR values for the progressive and regressive shoreline changes on the Navsari coast were 71.43 m/y & -70.95 m/y and 64.05 m/y & -65.46 m/y, respectively. The coastal stretch of the Navsari district is undergoing rapid changes, primarily at the mouth of the river basin. Misra and Balaji (2015) noted the shoreline change pattern along with the land use/land cover change of the coastal district and found a promising trend of accretion in the southernmost part near the Bhat coast. The gradual accumulation of sediment and sand over time is currently occupied by the dense mangroves/vegetation.

Valsad

The Valsad district is situated on the eastern side of the Gulf of Khambhat, which is the last coastal district of southern Gujarat. It has a long coastline that spans approximately 64 km. Forty percent of the coastline was accreted at minimum and maximum rates ranging from 0.01 to 81.39 m/y (LRR) but eroded at rates ranging from -0.01 to -195.65 m/y, while the remaining 11 km of the coast remained a stable coast. The average erosional NSM value is -185.42 m, while 82.34 m is the average accretion NSM value. Out of the 63.6 km long coastline, 35.6 km long coastline followed the low accretion and a low erosional pattern with no to minimal changes in the shoreline. Majorly, eroding and accreting transects were observed at the mouth of the river or at the opening of a small/large creek area along the district. This could be a result of various factors, such as the formation of sandbars, beach nourishment, sedimentation, or changes in local oceanic currents.

Union Territories

Two union territories i.e. Diu and Daman, each have a 12 km stretch of coastline, along with other coastal districts in Gujarat. According to recent findings, Diu has the most stable coast, with 85% of its coastline. On the other hand, only 36% (4.3 km) of the coastal area of Daman remained the same. Notably, both union territories have not experienced moderate to high erosion in the last 30 years. However, Daman has witnessed a low to high accretion of about 5.6 km during the same period.

Coastline modification factors: Coastal areas fluctuate due to a complex interplay of various natural and human-induced processes. The natural processes are influenced by the underlying geology and geomorphological changes including the action of waves and currents, fluctuations in sea level, sediment transportation, tectonic shifts, severe weather events, etc. These processes contribute to the gradual modification of shorelines over time, resulting in the formation of unique landforms that are shaped by natural forces. On the other hand, human activities can intensify the erosion of coastal areas and exacerbate this problem. These activities include the manipulation of hydrological cycles, mainly through dam construction, buildings and structures built on beaches, the construction of harbors, jetties, and other coastal structures, and the mining of beach sand and corals. All these factors can have a significant impact on the natural environment, and it is essential to balance human activities with the preservation of the natural ecosystem.

Overall, this research highlights the classified erosion and accretion trends to better understand the dynamics of coastal areas. Long-term coastal erosion patterns can lead to the loss of valuable land, damage to infrastructure, and increased vulnerability to natural disasters such as floods and storms. In contrast, accretion can help protect coastlines from erosion and provide important habitats for marine life and vegetation. These findings underscore the need for continued monitoring, research, and management efforts to ensure the long-term sustainability of the coastal area and the communities that depend on it.

Conclusion

The purpose of this study was to apply remote sensing and GIS tools/techniques to better understand the rate of district wise shoreline change. Erosion and accretion highly fluctuate in nature due to semidiurnal and mixed tides with high tidal ranges and regional hydrodynamics. Extensive mudflat regions are more prone to fluctuations due to their soft bottom sediments. This study attempted to track shoreline shifts along the coast of Gujarat for the past three decades from 1993 to 2023. This was a transect-based study in which statistics such as NSM, EPR, LRR, and WLR were calculated to evaluate the shoreline change rate. The present DSAS shoreline change analysis indicated that erosion occurred on 24% (207.6 km) of the total coast, whereas accretion was seen in 50% (436.5 km) of the transects. There were no notable alterations along the remaining 27% (234.1 km) of the stable coastline. Diu has continuously high coastal stability, while Devbhumi Dwarka and Gir Somnath have moderate coastal stability. Over the years, the coastal districts of Anand, Bharuch, Surat, and Ahmedabad have experienced significant accretion with little to no evidence of coastline stability. However, notable erosion was mostly observed on the southern coast of Gujarat on the coastlines of the Navsari and Valsad districts. This study was an effort toward continuous monitoring of shoreline change in coastal districts of Gujarat state along with the Union Territories. Utilization of remote sensing and GIS techniques can prove to be beneficial for the consistent and effective long-term monitoring of shoreline changes, especially in areas where manual field data collection is not practical. Ultimately, this study can assist local coastal managers, researchers, and decision-makers in evaluating the coastal changes that should be considered when developing coastal management plans for the Gujarat coast.

Peer Review: Externally peer-reviewed.

Author Contributions: Conception/Design of Study: FJ, KV.; Data Acquisition- FJ, KV.; Data Analysis/Interpretation FJ, KV.; Drafting Manuscript- FJ.; Critical Revision of Manuscript- FJ, KV.; Final Approval and Accountability- FJ. K.V.

Conflict of Interest: Authors declared no conflict of interest.

Financial Disclosure: Authors declared no financial support.

Acknowledgments: The satellite data downloaded from the United States Geological Survey are gratefully acknowledged. The authors would like to thank the anonymous reviewers for their insightful and constructive comments, which significantly contributed to the enhancement of the original manuscript.

Author Details

Foram Jadeja

[1] The Maharaja Sayajirao University of Baroda, Department of Environmental Studies, Faculty of Science, Gujarat, India

0000-0002-6609-8560 foram.jadeja-envphd@msubaroda.ac.in

Kauresh Vachhrajani

[2] The Maharaja Sayajirao University of Baroda, Department of Zoology, Faculty of Science, Gujarat, India

0000-0002-6840-4752

REFERENCES

Addo, K. A., Jayson-Quashigah, P. N., & Kufogbe, K. S. (2011). Quantitative analysis of shoreline change using medium resolution satellite imagery in Keta, Ghana. *Marine Science*, *1*(1), 1-9.

Alesheikh, A. A., Ghorbanali, A., & Nouri, N. (2007). Coastline change detection using remote sensing. *International Journal of Environmental Science & Technology*, *4*, 61-66.

Basheer Ahammed, K. K., Mahendra, R. S., & Pandey, A. C. (2016). Coastal vulnerability assessment for Eastern Coast of India, Andhra Pradesh by using geo-spatial technique. *Geoinformatics & Geostatistics: An Overview*, *4*(3).

Beluru Jana, A., & Hegde, A. V. (2016). GIS based approach for vulnerability assessment of the Karnataka coast, India. *Advances in Civil Engineering*, *2016*.

Braud, D. H., & Feng, W. (1998). Semi-automated construction of the Louisiana coastline digital land/water boundary using Landsat Thematic Mapper satellite imagery. *Louisiana Applied Oil Spill Research and Development Program, OS2 RAPD Technical Report Series*, *97*(002).

Burak, S., Dogan, E., & Gazioglu, C. (2004). Impact of urbanization and tourism on coastal environment. *Ocean & Coastal Management*, *47*(9-10), 515-527.

Çelik, O. İ., & Gazioğlu, C. (2020). Coastline difference measurement (CDM) method. *International Journal of Environment and Geoinformatics*, *7*(1), 1-5.

CERC. 1973. *Shore protection manual* (Vol. 1). US Army Coastal Engineering Research Center.

Chen, C., Bu, J., Zhang, Y., Zhuang, Y., Chu, Y., Hu, J., & Guo, B. 2019. The application of the tasseled cap transformation and feature knowledge for the extraction of coastline information from remote sensing images. *Advances in Space Research*, *64*(9), 1780-1791.

Coco, G., Senechal, N., Rejas, A., Bryan, K. R., Capo, S., Parisot, J. P., Brown, J.A. & MacMahan, J. H. (2014). Beach response to a sequence of extreme storms. *Geomorphology, 204*, pp.493-501.

Dey, M., Shanmuga Priyaa, S. & Jena, B. K. (2021) . A Shoreline Change Detection (2012-2021) and forecasting Using Digital Shoreline Analysis System (DSAS) Tool: A Case Study of Dahej Coast, Gulf of Khambhat, Gujarat, India. *Indonesian Journal of Geography*, *53*(2).

El-Asmar, H. M., & Hereher, M. E. (2011). Change detection of the coastal zone east of the Nile Delta using remote sensing. *Environmental Earth Sciences*, *62*, 769-777.

El-Sharnouby, B. A., El-Alfy, K. S., Rageh, O. S., & El-Sharabasy, M. M. (2015). Coastal changes along Gamasa beach, Egypt. *J Coast Zone Manag*, *17*, 393.

Feyisa, G. L., Meilby, H., Fensholt, R., & Proud, S. R. (2014). Automated Water Extraction Index: A new technique for surface water mapping using Landsat imagery. *Remote sensing of environment*, *140*, 23-35.

Frazier, P. S., & Page, K. J. (2000). Water body detection and delineation with Landsat TM data. *Photogrammetric engineering and remote sensing*, *66*(12), 1461-1468.

Gazioğlu, C. (2018). Biodiversity, coastal protection, promotion and applicability investigation of the ocean health index for Turkish seas. *International Journal of Environment and Geoinformatics*, *5*(3), 353-367.

Giardino, C., Bresciani, M., Villa, P., & Martinelli, A. (2010). Application of remote sensing in water resource management: the case study of Lake Trasimeno, Italy. *Water resources management*, *24*, 3885-3899.

Guariglia, A., Buonamassa, A., Losurdo, A., Saladino, R., Trivigno, M. L., Zaccagnino, A., and Colangelo, A. (2006). A multisource approach for coastline mapping and identification of shoreline changes.

Gupta, M. (2014). Monitoring shoreline changes in the Gulf of Khambhat, India during 1966–2004 using RESOURCESAT-1 LISS-III. *Open Journal of Remote Sensing and Positioning*, *1*(1), 27-37.

Himmelstoss, E., Henderson, R. E., Kratzmann, M. G., & Farris, A. S. (2018). *Digital shoreline analysis system (DSAS) version 5.0 user guide* (No. 2018-1179). US Geological Survey.

Hossain, M. S., Yasir, M., Wang, P., Ullah, S., Jahan, M., Hui, S., & Zhao, Z. (2021). Automatic shoreline extraction and change detection: A study on the southeast coast of Bangladesh. *Marine geology*, *441*, 106628.

Jayanthi, M., Thirumurthy, S., Samynathan, M., Duraisamy, M., Muralidhar, M., Ashokkumar, J., & Vijayan, K. K. (2018). Shoreline change and potential sea level rise impacts in a climate hazardous location in southeast coast of India. *Environmental monitoring and assessment*, *190*, 1-14.

Kabuth, A. K., Kroon, A., & Pedersen, J. B. (2014). Multidecadal shoreline changes in Denmark. *Journal of Coastal Research*, *30*(4), 714-728.

Kankara, R. S., Murthy, M. R., & Rajeevan, M. (2018). National Assessment of Shoreline changes along Indian Coast: Status report for 26 years (1990–2016). *NCCR Publication*.

Kumar, T. S., Mahendra, R. S., Nayak, S., Radhakrishnan, K., & Sahu, K. C. (2010). Coastal vulnerability assessment for Orissa State, east coast of India. *Journal of Coastal research*, *26*(3), 523-534.

Li, R. D., & Ma, R. (2001). The 4th International Symposium on Computer mapping and GIS for Coastal Zones Management–A comparative study of shoreline Mapping techniques. *Halifax, Nova Scotia, Canada*.

McFeeters, S. K. (1996). The use of the Normalized Difference Water Index (NDWI) in the delineation of open water features. *International journal of remote sensing*, *17*(7), 1425-1432.

Misra, A., & Balaji, R. (2015). Decadal changes in the land use/land cover and shoreline along the coastal districts of southern Gujarat, India. *Environmental Monitoring and Assessment*, *187*, 1-13.

Mohan, G. S., & Jairaj, P. G. (2014). Coastal vulnerability assessment along Kerala coast using remote sensing and GIS. *International Journal of Scientific & Engineering Research*, *5*(7), 228-234.

Mujabar, P. S., & Chandrasekar, N. (2013). Shoreline change analysis along the coast between Kanyakumari and Tuticorin of India using remote sensing and GIS. *Arabian Journal of Geosciences*, *6*, 647-664.

Nassar, K., Mahmod, W. E., Fath, H., Masria, A., Nadaoka, K., & Negm, A. (2019). Shoreline change detection using DSAS technique: Case of North Sinai coast, Egypt. *Marine Georesources & Geotechnology*, *37*(1), 81-95.

Pajak, M. J., & Leatherman, S. (2002). The high water line as shoreline indicator. *Journal of coastal research*, 329-337.

Pilkey, O. H., & Hume, T. M. (2001). The shoreline erosion problem: lessons from the past. *Water and Atmosphere*, *9*(2), 22-23.

Ratheesh, R., Rajput, P., Bhatti, H., Rajawat, A. S., and Rajak, D. R. (2023). Quantification of shoreline changes along the entire Indian coast using Indian Remote Sensing satellite images of 2004-06 and 2014-16. *Current Science (00113891)*, *124*(5).

Roy, S., Mahapatra, M., & Chakraborty, A. (2018). Shoreline change detection along the coast of Odisha, India using digital shoreline analysis system. *Spatial Information Research*, *26*, 563-571.

Santos, C. A. G., do Nascimento, T. V. M., Mishra, M., & da Silva, R. M. (2021). Analysis of long-and short-term shoreline change dynamics: A study case of João Pessoa city in Brazil. *Science of the Total Environment*, *769*, 144889.

Shen, L., & Li, C. (2010). Water body extraction from Landsat ETM+ imagery using adaboost algorithm. In *2010 18th International Conference on Geoinformatics* (pp. 1-4). IEEE.

Splinter, K. D., Turner, I. L., Davidson, M. A., Barnard, P., Castelle, B., & Oltman-Shay, J. (2014). A generalized equilibrium model for predicting daily to interannual shoreline response. *Journal of Geophysical Research: Earth Surface*, *119*(9), 1936-1958.

Sutariya, S., Hirapara, A., Meherbanali, M., Tiwari, M. K., Sıngh, V., & Kalubarme, M. (2021). Soil moisture estimation using Sentinel-1 SAR data and land surface temperature in Panchmahal district, Gujarat State. *International Journal of Environment and Geoinformatics*, *8*(1), 65-77.

Thieler, E. R., Himmelstoss, E. A., Zichichi, J. L., & Ergul, A. (2009). *The Digital Shoreline Analysis System (DSAS) version 4.0-an ArcGIS extension for calculating shoreline change* (No. 2008-1278). US Geological Survey.

Tran Thi, V., Tien Thi Xuan, A., Phan Nguyen, H., Dahdouh-Guebas, F., & Koedam, N. (2014). Application of remote sensing and GIS for detection of long-term mangrove shoreline changes in Mui Ca Mau, Vietnam. *Biogeosciences*, *11*(14), 3781-3795.

Ustun, B., Ekercin, S., & Musaoglu, N. (2004). A performance analysis of the classification and manual digiting methods for the detection of coast line by using satelllite image data. *Remote sensing in transition*, 143-148.

Vitousek, S., Barnard, P. L., Limber, P., Erikson, L., & Cole, B. (2017). A model integrating longshore and cross-shore processes for predicting long-term shoreline response to climate change. *Journal of Geophysical Research: Earth Surface*, *122*(4), 782-806.

Xu, H. 2006. Modification of normalised difference water index (NDWI) to enhance open water features in remotely sensed imagery. *International journal of remote sensing*, *27*(14), 3025-3033.

Yan, D., Yao, X., Li, J., Qi, L., & Luan, Z. (2021). Shoreline change detection and forecast along the Yancheng coast using a digital shoreline analysis system. *Wetlands*, *41*, 1-16.